

1 **Irrigation decision support based on leaf relative water content**
2 **determination in olive grove using near infrared spectroscopy**

3

4

5

6 **Irina Torres^a, María-Teresa Sánchez^{a*}, María Benlloch-González^b, Dolores Pérez-**
7 **Marín^{c,*}**

8

9 ^aDepartment of Food Science and Food Technology, Faculty of Agricultural and Forestry
10 Engineering, University of Cordoba, Campus Rabanales, E-14071 Cordoba, Spain

11 ^bDepartment of Agronomy, Faculty of Agricultural and Forestry Engineering, University
12 of Cordoba, Campus Rabanales, E-14071 Cordoba, Spain

13 ^c Department of Animal Production, Faculty of Agricultural and Forestry Engineering,
14 University of Cordoba, Campus Rabanales, E-14071 Cordoba, Spain

15

16

17

18

19

20 * Corresponding authors at: Campus Rabanales, E-14071 Cordoba, Spain. Tel.: +34 957
21 212576; fax: +34 957 212000.

22

23 E-mail addresses: teresa.sanchez@uco.es (M.T. Sánchez) and dcperez@uco.es (D. Pérez-

24 Marín)
25

26 **ABSTRACT**

27 The relative water content (RWC) provides a measurement of the water deficit of the leaf
28 and may indicate a degree of stress endured under conditions of drought and high
29 temperatures, its measurement therefore, being essential for the appropriate management
30 of irrigation. This study sought to ascertain the viability of near infrared spectroscopy
31 (NIRS), using a handheld portable NIR instrument for the non-destructive and *in situ*
32 determination of RWC in olive tree leaves cultivated under higher temperatures than
33 ambient. Different combinations of pre-treatments and first and second derivative were
34 assayed to obtain information of spectral data and to develop calibration models. A
35 calibration equation with enough prediction performance for supporting irrigation
36 decision-making (standard error of cross-validation, SECV = 1.52%; $r^2_{cv} = 0.61$; residual
37 predictive deviation for cross-validation, $RPD_{cv} = 2.01$) was obtained. The findings
38 obtained from the external validation of the model (standard error of prediction, SEP =
39 1.63%; $r^2_p = 0.64$; residual predictive deviation for prediction, $RPD_p = 2.17$) suggest the
40 viability of the on-tree use of NIRS technology for the instant measurement of RWC in
41 olive groves, ensuring a major saving in time and avoiding the disadvantage of
42 transporting samples to the lab, thereby favouring real-time decision-making in the field
43 regarding the optimal amounts of irrigation to be applied; this is of enormous significance
44 for the future, given that the availability of irrigation water for such vital crops to the
45 Mediterranean region as the olive could be limited in years to come by a gradual increase
46 in planetary temperatures.

47

48 *Keywords:* Olive grove; *In situ* RWC measurement; NIRS technology; Irrigation
49 management; Climate change

50

51

52 **1. Introduction**

53

54 Olive (*Olea europaea* L.) is the most prevalent crop in the Mediterranean basin and has
55 enormous ecological and economic importance to the region. It is well suited to the
56 Mediterranean climate, which is characterised by hot and dry summers, mild winters, and
57 relative lack of rainfall. However, the climatic conditions of this region are expected to
58 change in the near future due to global warming. Climate experts have predicted an
59 increase in average air temperature in the range of 2–5°C (Giorgi, 2006; Gualdi et al.,
60 2013; IPCC, 2014) together with more frequent occurrence of extreme events such as
61 droughts and heat-waves (Giorgi & Lionello, 2008; Tanasijevic, Todorovic, Pereira,
62 Pizzigally, & Lionello, 2014). In the climatic conditions being predicted for the region
63 therefore – lower precipitation and higher temperatures – it is likely that this species will
64 undergo frequent periods of water and heat stress, with concomitant effects on yields.

65 The leaf is the organ of the olive tree that is most responsive to environmental
66 conditions (Nevo et al., 2000). The RWC of a leaf is an important indicator of a plant's
67 water status. In this sense, RWC provides a measurement of the 'water deficit' of the leaf
68 and may indicate a degree of stress expressed under unfavourable conditions such as
69 drought or high temperature (Barrs & Weatherley, 1962; Barrs, 1968). This parameter
70 has long been used as a reliable indicator of plant wellbeing and could be highly useful
71 in ascertaining whether olive trees subjected to the climate conditions of the future are
72 suffering from stress at any of the phenological stages of their reproductive cycle (Mullan
73 & Pietragalla, 2012; Rallo & Cuevas, 2017). It can be useful for indicating plant water
74 needs (Jones, 2004, 2007) aimed at reducing potential stressful situations for olive trees,

75 especially in those phenological stages where the species is more vulnerable to extreme
76 conditions.

77 The traditional method used to determine RWC is by measuring the differences in
78 weight between the fresh, dry and turgid leaf (Stocker, 1929). This method is time-
79 consuming– it requires more than 24 hours – and labour intensive in the laboratory.
80 Moreover, although the procedure is straightforward, the taking of samples is prone to
81 errors, because it can be accompanied by a modification in the water content prior to the
82 start of the analysis. There is therefore a need for a fast and efficient method for the
83 determination of the RWC in a way that is non-destructive and *in situ* (on-tree), allowing
84 growers to make accurate irrigation decisions depending on the water deficit of the tree.
85 In this context, near-infrared spectroscopy has significant potential as an appropriate
86 method, since it is a non-invasive, rapid, economical and accurate alternative to traditional
87 methods. The technology is simple, so fewer errors are introduced than in conventional
88 analytical techniques (Osborne, Fearn, & Hindle, 1993). At the same time, NIR
89 spectroscopy is a powerful tool for general process monitoring in real time (De la Roza
90 et al., 2017; Zhang et al., 2017); this is of particular interest for many agricultural practices
91 such as irrigation.

92 NIRS technology has been successfully used to determine various parameters in
93 the leaves of a range of species, using both laboratory (Menesatti et al., 2010; Fernández-
94 Martínez et al., 2017) and portable equipment (Itoh, Tomita, Uno, & Naomasa, 2011;
95 Steidle-Neto, Lopes, Pinto, & Zolnier, 2017). In the case of olive leaves, the research that
96 has been published makes reference to measuring nutrient content (Fernández-Cabanás,
97 Garrido-Varo, Delgado-Pertiñez, & Gómez-Cabrera, 2008; Rotbart et al., 2013) and
98 differentiation between juvenile and adult leaves (León & Downey, 2006), both carried
99 out in laboratory conditions. However, there is no trace in the scientific literature of any

100 research into the measurement of RWC in olive leaves using NIRS technology. Several
101 authors have demonstrated the feasibility of NIRS technology in the non-destructive
102 measurement of RWC in the fresh leaves of *Epipremnum aureum* and *Miscanthus* (*M.*
103 *sinensis*, *M. sacchariflorus*, *M. lutarioriparia*, *M. floridulus* and *M. giganteus*) (Zhang,
104 Li, & Zhang, 2012; Jin, Shi, Yu, Yamada, & Sacks, 2017) using lab-based
105 monochromator instruments, and in seedling eucalyptus leaves using a portable MEMS-
106 NIRS instrument (Warburton, Brawner, & Meder, 2014).

107 The aim of this study was to evaluate the feasibility of using NIRS technology for
108 determining RWC in olive leaves growing *in situ*. The goal is to help growers to make
109 irrigation decisions to mitigate negative effects of stress on crop performance under future
110 weather conditions associated to climate change.

111

112 **2. Material and methods**

113

114 *2.1. Plant material*

115

116 Olive (*Olea europaea* L.) leaves from cultivars ‘Picual’ (N = 178 samples) and
117 ‘Arbequina’ (N = 72 samples) were analysed. Each sample consisted of four fully-
118 expanded leaves, which were located at the middle position of the canopy and exposed to
119 sunlight. Samples were sequentially collected from March 2016 to July 2017 on 17
120 different days, covering the range of the distinct phenological phases of the olive tree
121 (Table 1).

122 These olive trees were located in an experimental field at the Rabanales Campus
123 of Córdoba University (Spain) and exposed to different temperature treatments (ambient
124 temperature *versus* 4 °C above ambient temperature), by the use of open top chambers

125 equipped with heating and ventilation devices. These systems are able to maintain
126 permanently a day/night temperature gradient between the tree and the surrounding
127 environment of 4 °C throughout the complete reproductive cycle of this species
128 (Benlloch-González, Sánchez-Lucas, Benlloch, & Fernández-Escobar, 2018).

129

130 2.2. *NIRS analysis*

131

132 A handheld Micro-Electro-Mechanical System (MEMS) spectrometer
133 (MicroPHAZIR™, Thermo Fisher Scientific, Wilmington, MA, USA) was used to collect
134 the spectra of olive leaves *in-situ*. This instrument operates in reflectance mode (log 1/R)
135 across the spectral range of 1600–2400 nm every 8 nm. Internal white reference was
136 automatically collected every ten minutes.

137 Olive tree leaves are small and thick, so in order to avoid the loss of light during
138 spectra collection and to ensure that the field analysis was carried out correctly, without
139 detaching the leaf from the tree, a circular-(15 cm of diameter) black metal plate was used
140 to hold the leaf.

141 At first, with the aim of establishing which side of the leaf was most appropriate
142 for recording spectra, NIRS readings were carried out both on the adaxial and abaxial side
143 of the leaf. Three spectral measurements were made per leaf (at the upper, middle and
144 bottom parts) and per side (adaxial and abaxial). Since, four leaves were analysed per
145 each olive tree, and a total of 12 spectra were obtained for each sample and for each leaf
146 side. These 12 spectra per side were averaged to provide a mean spectrum for each olive
147 tree, a mean for each sample and, initially, for each side.

148

149 2.3. *Reference method*

150

151 RWC was determined in accordance with the procedure set out by Stocker (1929).
152 Briefly, leaves were collected at solar noon and quickly put inside a 10 ml-test tube, which
153 was hermetically sealed with a lid and placed in a container filled with ice to avoid loss
154 of leaf moisture. Once in the laboratory, the olive leaves were weighed (FW) and then
155 rehydrated by adding 1 ml of deionised water to the test tube. After incubation at 4 °C for
156 24 h, the leaves were re-weighed to determine the turgid weight (TW) and thereafter put
157 into an oven at 70 °C for 48 h to determine the dry weight (DW). The leaf RWC (%) was
158 calculated as follows:

$$159 \quad RWC (\%) = ((FW-DW)/(TW-DW)) \times 100$$

160 For the purposes of this research the Standard Error of Laboratory (SEL) was
161 estimated by analysing 10 duplicated samples. In order to calculate the error, both the
162 sampling error (selection of two consecutive leaves to analyse) and the error arising from
163 the process of analysis in the laboratory (analysis was done by duplicated) were
164 determined. Once these two errors had been calculated, the SEL value was obtained in
165 accordance with Fearn (1986).

166

167 2.4. Spectral repeatability

168

169 The spectral repeatability was evaluated using the root mean squared (RMS) statistic, is
170 defined as the averaged root mean square of differences between the different subsamples
171 scanned at n wavelengths (Shenk & Westerhaus, 1995a, 1996). It indicates the similarity
172 between different spectra of a single sample, in this case between the three spectra
173 collected per sample. For this purpose, 10 leaves were selected from which three spectra
174 were taken in the upper, middle and lower parts using the MEMS-NIR instrument.

175 An admissible limit for spectrum quality and repeatability was set following the
176 procedure described by Martínez, Garrido, De Pedro and Sánchez, (1998) to calculate the
177 standard deviation (STD) limit from the RMS statistic and obtain an RMS cut-off value.

178

179 2.5. *Data processing*

180

181 2.5.1. *Principal component analysis*

182

183 With the goal of studying the relationship between the RWC and the distinct phenological
184 states in the olive tree's cycle, as well as conducting the possible identification of
185 anomalous samples, Principal Component Analysis (PCA) was carried out. In this work,
186 PCA was performed using the mean spectrum derived from each of the days being
187 analysed. Matlab software (version 2015a, The Mathworks, Inc., Natick, Massachusetts,
188 US) was used to conduct PCA, using mean centre, which subtracts the mean spectrum of
189 the group from each spectrum, as a pre-treatment (Wise et al., 2006).

190

191 2.5.2. *Selection of the calibration and validation sets*

192

193 Data pre-processing and chemometric treatments were performed using the WinISI
194 software package ver. 1.50 (Infrasoft International LLC, Port Matilda, PA, USA). For the
195 development of the model, the total set was divided into a calibration and a validation set.
196 The selection of these sets was based on spectral information, using the CENTER
197 algorithm (Shenk & Westerhaus, 1995a).

198 As spectral pre-treatments, Standard Normal Variate (SNV) and Detrending (DT)
199 were used to remove scatter interferences (Barnes, Dhanoa, & Lister, 1989) together with

200 the first derivative treatment '1,5,5,1', where the first digit is the number of the derivative,
201 the second is the gap over which the derivative is calculated, the third is the number of
202 data points in a running average or smoothing, and the fourth is the second smoothing
203 (Shenk & Westerhaus, 1995b).

204 Having ordered the population by spectral distances, samples that displayed GH
205 values > 3 were removed. The validation set was selected by taking one sample out of
206 every four in the initial set; the remainder constituted the calibration set.

207

208 2.5.3. Calibration development and validation procedure

209

210 Calibration models for the prediction of the RWC of the olive leaf were developed using
211 Modified Partial Least Squares (MPLS) regression (Shenk & Westerhaus, 1995a) with
212 six cross-validation groups to avoid overfitting. SNV and DT and Multiplicative Scatter
213 Correction (MSC) were used as pre-processing for scatter correction (Barnes et al., 1989;
214 Dhanoa, Lister, Sanderson, & Barnes, 1994). Additionally, four derivative mathematical
215 treatments were tested: 1,5,5,1; 1,10,5,1; 2,5,5,1; and 2,10,5,1.

216 Best equations were selected according to the following statistics: coefficient of
217 determination for calibration (r^2_c), standard error of calibration (SEC), coefficient of
218 determination for cross-validation (r^2_{cv}) and standard error of cross-validation (SECV).
219 However, in order to standardise the SECV value, another statistic, the residual predictive
220 deviation (RPD), calculated as the ratio between the standard deviation (SD) of the
221 calibration set to the SECV, was also calculated.

222 The best model obtained for the calibration set, as selected by statistical criteria,
223 was subjected to external validation and evaluated in accordance with the protocol
224 outlined by Windham, Mertens, and Barton (1989).

225

226 3. Results and discussions

227

228 3.1. Optimisation of in-situ olive tree analysis

229

230 After the spectra taken from both sides of the leaf at the beginning of the study, it was
231 decided to take spectra only from the adaxial side, because the leaf of the olive has a
232 highly-pronounced central vein on the abaxial side, causing greater dispersion of light
233 during analysis. The procedure of taking spectra only from the adaxial side of the leaf is
234 consistent with the practice of such authors as Zhang et al. (2012) in *Epipremnum aureum*,
235 and Warburton et al. (2014) and Yang et al. (2017). in *Eucalyptus* leaves. Specifically,
236 the study carried out by Warburton et al. (2014) on *Eucalyptus* seedlings, aimed at
237 determining which side of the leaf was most appropriate for NIRS analysis, concluded
238 that there were no significant differences enabling a particular part of the leaf to be
239 established for recording spectra, although it is important to note that *Eucalyptus* leaves
240 do not exhibit the very prominent central vein that is a feature of olive leaves.

241 After that and prior to the model development, it was necessary to optimise the
242 NIRS analysis by means of the spectrum quality and repeatability measurement.

243 Firstly, the existence of noise in the spectrum was evaluated (spectral range 1600–
244 2400 nm). To this end, the derivative treatment 1,1,1,1 was applied in order to determine
245 the area of the spectral range affected by noise, given that it degrades the signal/noise
246 relationship (Hruschka, 2001). After this process, the spectral range between 2312–2400
247 nm was eliminated (Fig. 1).

248 Secondly, spectral repeatability which is crucial to the construction of models that
249 are both accurate and robust was evaluated. Statistical methods such as defined RMS cut-

250 off limit can be useful for this purpose. The RMS cut-off was calculated as described in
251 Section 2.4.

252 The STD_{limit} for the samples analysed using the handheld instrument was 42,663
253 $\mu\log(1/R)$. Despite the importance of this parameter for fine-tuning new analytical
254 methodologies and ensuring more robust models, no references have been found in the
255 scientific literature that calculate STD_{limit} for the *in situ* analysis of olive leaves. In the
256 present research, any sample whose triplicated screening scans yielded an RMS above
257 this value was eliminated and repeated until values fell below that limit, thus ensuring a
258 high degree of spectrum repeatability. It was found for example that the samples taken on
259 16 March 2017 exhibited values far higher than the established STD_{limit} , despite the
260 analysis of the leaves being repeated on numerous occasions. A detailed study was carried
261 out of the various factors that could have affected the analysis on that day, arriving at the
262 conclusion that the variation arose from the fact that a few days prior to the analysis a
263 copper-based treatment was been applied, with the consequence that the particles
264 deposited on the leaves caused the analysis to be distorted. The samples taken on that
265 particular day were therefore eliminated, leaving a set consisting of the 235 remaining
266 samples.

267

268 3.2. *Principal Component Analysis (PCA)*

269

270 PCA was performed on the set comprising the spectra recorded per day ($N = 16$), after
271 eliminating those mentioned in section 3.1. Figure 2a shows the PCA loadings for intact
272 olive leaves in the spectral range 1600–2312 nm, while Fig. 2b displays scores of the
273 second and third components of the PCA model. These two components were chosen
274 because although the first two principal components (PC1 and PC2) represented a high

275 proportion of the explained variance (82.23% and 16.57%, respectively), they did not
276 facilitate the grouping of the samples in accordance with the phenological state; this
277 grouping does however seem to become evident when the latent variables PC2 and PC3
278 are used.

279 The graphic representation of the loadings for PC2 and PC3 shows that the main
280 absorption peaks for differentiating between the various phenological states of the olive
281 tree are those related to water and carbohydrates respectively. Whereas the PC2 weighting
282 coefficient exhibits a peak of water around 1900 nm, PC3 exhibits a band that is
283 characteristic of carbohydrates (~1780 nm) (Shenk et al., 2008). The accumulation of
284 carbohydrates in the plant differs in accordance with the phenological state that the plant
285 is in at that time; thus, during the period of fruit formation and ripening; nutrients and
286 carbohydrates will migrate from the leaf towards the fruit, accumulating in the latter
287 (Fernández-Escobar, Moreno, & García-Creus, 1999). It therefore follows that the
288 carbohydrate content in the leaf, represented by the third principal component, aids
289 discrimination between the states the plant happens to be in.

290 Score plotting revealed apparent grouping by phenological stages (Fig. 2b), as
291 shown in Table 1. Six groups emerge, which range from the period of winter dormancy
292 to the maturation of the fruit, encompassing the intermediate phases of flowering, setting
293 and growth of the fruit (Rallo & Cuevas, 2017).

294 In light of the PCA scores and bearing in mind the data set out in Table 1, it may
295 be said that the phases of winter dormancy and flowering, which fundamentally occurs
296 during the spring, when evapotranspiration is low (a rainy season), are related to PC2.
297 The negative PC2 scores are associated with times of restricted water, which place the
298 plants in situations of more acute hydrological stress. As it has already been mentioned,
299 PC3 may be linked to carbohydrate content. This becomes particularly evident when

300 analysing the group pertaining to the swelling of the fruit, which exhibits a positive PC3
301 score (Fig. 2b), setting it apart from the other samples and highlighting that in this phase
302 there is a movement of carbohydrates from the plant's various organs towards the fruit,
303 where it is subsequently assimilated (Fernández-Escobar et al., 1999).

304 León and Downey (2006) used PCA to differentiate between young and adult
305 leaves in olive trees. They proposed that water content and various chemical compounds,
306 particularly pigments, were responsible for this separation between the various ages of
307 the leaf. In accordance with these authors, the distinction between the various
308 phenological states could be due to the water and carbohydrate content of the leaf,
309 although a depth study of the spectral characteristics of each state of the plant should be
310 considered in future research.

311

312 3.3. *Population characterisation*

313

314 After applying the CENTER algorithm to the overall set (N = 235), two samples were
315 identified as anomalous spectra. Once spectral outliers were removed, a set consisting of
316 233 samples was used to develop calibration models. As described in section 2.5, the set
317 was divided into a training set (N = 174) and a test set (N = 59).

318 The distribution and statistics of the calibration and validation sets (mean, SD and
319 CV) for the RWC are shown in Fig. 3. The structured selection based only on the spectral
320 information treatments, such as CENTER algorithm, proved to be useful because the
321 statistics for both sets were similar and the range in the calibration set encompassed the
322 validation set.

323 Although *a priori* it may seem that the RWC parameter exhibits a wide range,
324 both for the calibration (77.23–96.24 %) and for the validation set (78.22–95.61 %), this

325 parameter actually exhibits severely restricted variability, as is evident from the low
326 coefficients of variation obtained (Fig. 3). For the calibration set, 93% of the samples
327 recorded an RWC of between 85% and 95%, while in the validation set 88% of the
328 samples fell within this range, with very few samples (9 out of 174 and 5 out of 59 for the
329 calibration and validation sets, respectively) recording RWC scores below 85%.

330 The low variability ($CV_c = 3.37\%$ and $CV_v = 3.95\%$) is due to the RWC in olive-
331 tree leaves not subjected to controlled water stress being around 90-95%, so this variation
332 only derives from periods in which olives are suffering from water stress. Olive trees are
333 drought tolerant, and leaves can reach extremely low relative water contents (75-80%)
334 before losing turgor (Lo Gullo & Salleo, 1988). Therefore, values below 80% may
335 correspond to extreme temperature events, which generally occur during the long dry
336 season of the Mediterranean areas, where symptoms of dehydration are frequently
337 observed and are generally associated with a low-potassium nutritional status (Fernández-
338 Escobar, García, & Benlloch, 1994), something that was not applicable in the case of the
339 current trial.

340

341 3.4. *Calibration and validation for the prediction of the relative water content*

342

343 Statistics for the best models obtained using the various pre-treatments to determine RWC
344 in olive leaves measured on-tree are shown in Table 2.

345 According to Shenk and Westerhaus (1996) and Williams (2001), all models
346 obtained enable classification of the RWC parameter between high, medium and low
347 values ($0.50 < r^2_{cv} < 0.69$), being the best of them the one obtained using MSC and the
348 first derivative of the spectrum ($SECV = 1.52\%$; $r^2_{cv} = 0.61$; $RPD_{cv} = 2.01$).

349 In the present study, the estimated SEL was 0.87%. According to Fearn (1986),
350 the SECV is determined not only by the SEL but also reflects the error of the NIRS
351 method and the chemometric method. If the value of SECV is less than two times the SEL
352 of the reference method, the NIRS equation is fit for use (Windham et al., 1989), meaning
353 that this would be considered as appropriate for use in the field.

354 In order to compare the results obtained here to those obtained by other authors in
355 leaves, the RPD_{cv} statistic was used to standardise the SECV value.

356 No other results have been found for determining RWC in olive leaves. However,
357 various authors have used the technique to determine this parameter in a range of crops,
358 initially using monochromator instruments in the laboratory. Zhang et al. (2012) reported
359 good predictive capability ($RPD_{cv} = 2.73$) in determining the RWC in *Epipremnum*
360 *Aureum* subjected to various water stress treatments, using a monochromator instrument
361 with a spectral range of 200–1100 nm and a resolution of 1 nm. Jin et al. (2017) reported
362 superior results to those obtained here ($RPD_{cv} = 2.75$) for *Miscanthus* leaves, using a
363 monochromator instrument for the NIRS analysis with a wide spectral range (400–2500
364 nm, every 2 nm). These authors also had a calibration set for the parameter being studied
365 that exhibited greater variability ($CV = 6.53\%$), compared to the present case ($CV =$
366 3.37%), something that enables more robust models to be obtained (Shenk, Westerhaus,
367 & Berzaghi, 1997). It is important to point out that both studies mentioned above carried
368 out their RWC determinations with NIRS in the laboratory, whereas in the present study
369 the analysis was conducted directly on the tree, with the MEMS-NIR instrument
370 previously described. Moreover, the difference in predictive capacity between the first
371 two spectrophotometers and the handheld instrument may reflect differences in spectral
372 ranges, spectral resolution and in measuring area; the MEMS device measures an area of
373 only around 4 mm², whereas both monochromators scan the whole sample.

374 While there are no reports of the use of portable instruments to measure RWC in
375 olive leaves, various authors have used this type of instrument to measure RWC in the
376 leaves of *Eucalyptus* seedlings. Thus, Warburton et al. (2014) measured RWC using a
377 MEMS-NIR (MicroPhazir™ NIR spectrometer) instrument in the 1600–2400 nm spectral
378 range; the results were better ($r^2_{cv} = 0.88$ and RER = 10.45) than those obtained here (r^2_{cv}
379 = 0.61 RER = 12.51), possibly owing to the fact that they had a calibration set with a
380 greater range (15.40–99.30%) than the one in the present study (77.23–96.24%).
381 According to Fearn (2014), although r^2_{cv} can be useful for studying the predictive
382 capability of the model, this is closely linked to the range of reference values, and this
383 may provide a reason why the aforementioned authors reported a higher determination
384 coefficient than that obtained here. In a similar trial and using a NIRS instrument that
385 worked in the same spectral range (1600–2400 nm), Yang et al. (2017) obtained, for the
386 *in situ* measurement of RWC in *Eucalyptus* seedlings, a predictive capability model
387 (RPD_c = 2.59) that was slightly higher to the one obtained here (RPD_c = 2.09). This may
388 be due to the fact that the authors in question had a calibration set with greater variability
389 (SD = 6.33% and CV = 7.9%) than that in the present study (SD = 3.05% and CV =
390 3.37%), as well as the difficulties implicit in olive leaves in terms of thickness, sheen,
391 enervation, etc., compared to *Eucalyptus* leaves, something that may have effect on NIRS
392 analysis.

393 It should be noted that all these authors have conducted their experiments under
394 controlled environmental conditions (temperature, humidity, irrigation, etc.), with
395 situations involving induced water stress, thereby ensuring a set with a good and even
396 coverage of the range. As Pérez-Marín, Garrido-Varo, and Guerrero (2005) point out, the
397 distribution of samples within the calibration set is of great importance, because a uniform

398 distribution throughout the range of the parameter being studied helps to obtain robust
399 models.

400 Finally, Fig. 4 shows the regression coefficients for the best predictive model for
401 the RWC parameter. The figure illustrates that the areas of the spectrum with greater
402 weight in the model are located around 1720 nm, related to the C-H stretch first overtone
403 and around 1936 nm, which corresponds to O-H bend second overtone (Osborne et al.,
404 1993). This makes sense, because the RWC in olive leaves is very high, at around 90-
405 95%. Furthermore, the area at around 2200 nm could be attributed to the C=O second
406 overtone (Shenk, Workman & Westerhaus, 2008).

407

408 3.5. *External validation procedure*

409

410 After the development and analysis of the calibration models, the best model was
411 subjected to external validation. For this purpose, a sample set not included in the
412 calibration was used. Validation was performed using a set initially comprising 59
413 samples. Prior to the validation procedure, four samples were excluded from the
414 validation set because they displayed values of RWC (78.22, 79.08, 95.60 and 95.61%)
415 beyond the range obtained after the development of the equation (83.34–95.42%) for the
416 parameter analysed. A graphic representation of the reference values *versus* the NIR
417 predicted values for RWC in olive leaves is shown in Fig. 5.

418 The model developed for the prediction of the RWC complies with the limit
419 established in terms of r^2_p for its implementation in routine ($r^2_p > 0.60$), as well as the
420 confidence control limits for bias and SEP(c). The SEP value obtained shows a minor
421 difference (0,09 %) compared to the SECV, and around 0.12% compared to the mean of
422 the parameter, thereby confirming that the SECV provides a good estimate of the SEP

423 (Shenk et al., 2008). In addition, the slope (slope = 1.09) also falls within the established
424 slope values (0.90–1.1) (Windham et al., 1989).

425 These findings suggest that the NIRS equation obtained may be considered as a
426 first step for the *in situ* measurement of RWC in olive leaves. This could eventually enable
427 growers to ascertain the plant's degree of water stress in real time, and to take appropriate
428 and informed decisions about the irrigation of the crop.

429 Under future scenarios, growers could use leaf RWC measures by NIRS
430 technology to quickly determine *in situ* whether olive is suffering from water shortage,
431 trying to prevent stressful conditions and supporting irrigation scheduling.

432 In a practical sense, the best strategy to follow is to make a protocol in which the
433 value of RWC corresponding to each phenological stage and specie is established. Values
434 of leaf RWC rapidly measured using NIRS technology which were below those indicate
435 that irrigation treatments would be necessary. This would be an excellent complement to
436 the different routine scanning usually made, such as soil water content and tree
437 evotranspiration demand.

438

439 **4. Conclusions**

440

441 The results of this study, which used a handheld NIR spectrophotometer, confirmed the
442 viability of NIRS technology for the measurement of RWC in olive leaves on the tree.
443 Non-destructive and rapid determination of this parameter provides a quantitative
444 measure of the hydration status of the olive tree in the field, enabling optimal and precise
445 management of irrigation, something that will prove of great importance to olive
446 cultivation in Mediterranean countries. Climate change forecasts are predicting major
447 periods of drought and an increase in temperatures in the region, where water will become

448 an increasingly scarce resource; this will make it imperative to be able to determine the
449 RWC of olive trees with a view to maintaining the efficiency of photosynthesis and crop
450 productivity.

451 Over the coming years, further studies will be needed in order to improve the
452 calibration specificity, accuracy and robustness of this procedure.

453

454 **Acknowledgement**

455

456 The authors would like to thank Ms. M^a Carmen Fernández for her technical support.

457 Furthermore, the authors wish to express their gratitude to the Spanish Ministry of

458 Education, Culture and Sports for the support offered to Irina Torres Rodríguez in the

459 form of the Training programme for Academic Staff (FPU).

460

461 **REFERENCES**

462

463 Barnes, R.J., Dhanoa, M.S., & Lister, S.J. (1989). Standard Normal Variate

464 Transformation and De-trending of near infrared diffuse reflectance spectra.

465 *Applied Spectroscopy*, 43, 772–777.

466 Barrs, H.D. (1968). Determination of water deficits in plant tissues. In T. T. Kozlowski,

467 (Ed.), *Water deficits and plant growth* (Vol. 1, pp. 235–368). New York:

468 Academic Press.

469 Barrs, H.D., & Weatherley, P.E. (1962). A re-examination of the relative turgidity

470 technique for estimating water deficits in leaves. *Australian Journal of Biological*

471 *Sciences*, 15, 413–428.

472 Benlloch-González, M., Sánchez-Lucas, R., Benlloch, M., & Fernández-Escobar, R.
473 (2018). An approach to global warming effects on flowering and fruit set of olive
474 trees growing under field conditions. *Scientia Horticulturae*, 240, 405–410.

475 De la Roza-Delgado, B., Garrido-Varo, A., Soldado, A., Arrojo, A.G., Valdés, M.C.,
476 Maroto, F., & Pérez-Marín, D. (2017). Matching portable NIRS instruments for
477 *in situ* monitoring indicators of milk composition. *Food Control*, 76, 74–81.

478 Dhanoa, M.S., Lister, S.J., Sanderson, R., & Barnes, R.J. (1994). The link between
479 Multiplicative Scatter Correction (MSC) and Standard Normal Variate (SNV)
480 transformations of NIR spectra. *Journal of Near Infrared Spectroscopy*, 2, 43–47.

481 Fearn, T. (1986). Some statistical comments on the errors in NIR calibrations. *Analytical*
482 *Proceedings Articles*, 23, 123–125.

483 Fearn, T. (2014). The overuse of R^2 . *NIR News*, 25–32.

484 Fernández-Cabanás, V.M., Garrido-Varo, A., Delgado-Pertíñez, M., & Gómez-Cabrera,
485 A. (2008). Nutritive evaluation of olive tree leaves by near-infrared spectroscopy:
486 effect of soil contamination and correction with spectral pretreatments. *Applied*
487 *Spectroscopy*, 62, 51–58.

488 Fernández-Escobar, R., García, T., & Benlloch, M. (1994). Estado nutritivo de las
489 plantaciones de olivar en la provincia de Granada. *ITEA*, 90, 39–49.

490 Fernández-Escobar, R., Moreno, R., & García-Creus, M. (1999). Seasonal changes of
491 mineral nutrients in olive leaves during the alternate-bearing cycle. *Scientia*
492 *Horticulturae*, 82, 25–45.

493 Fernández-Martínez, J., Joffre, R., Zacchini, M., Fernández-Marín, B., García-Plazaola,
494 J.I., & Fleck, I. (2017). Near-infrared reflectance spectroscopy allows rapid and
495 simultaneous evaluation of chloroplast pigments and antioxidants, carbon isotope

496 discrimination and nitrogen content in *Populus* spp. leaves. *Forest Ecology and*
497 *Management*, 399, 227–234.

498 Giorgi, F. (2006). Climate change hot-spots. *Geophysical Research Letter*, 33, L08707,
499 1–4.

500 Giorgi, F., & Lionello, P. (2008). Climate change projections for the Mediterranean
501 region. *Global and Planetary Change*, 63, 90–104.

502 Gualdi, S., Somot, S., Li, L., Artale, V., Adani, M., Bellucci, A., Braun, A., Calmanti, S.,
503 Carillo, A., Dell’Aquila, A., Déqué, M., Ruti, C., Sanna, A., Sannino, G.,
504 Scoccimarro, E., Sevault, F., & Navarra, A. (2013). The CIRCE simulations:
505 regional climate change projections with realistic representation of the
506 Mediterranean Sea. *Bulletin of the American Meteorological Society*, 94, 65–81.

507 Hruschka, W.R. (2001). Data analysis: Wavelength selection methods. In P.C. Williams,
508 & K.H. Norris (Eds.), *Near-infrared technology in the agricultural and food*
509 *industries* (pp. 35-55). St. Paul, MN: AACC, Inc.

510 Intergovernmental Panel on Climate Change (IPCC). (2014). Climate change 2014:
511 Synthesis Report. In R.K. Pachauri & L.A. Meyer (Eds.), *Contribution of working*
512 *groups I, II and III to the fifth assessment report of the intergovernmental panel*
513 *on climate change* (pp. 151). Geneva, Switzerland: IPCC.

514 Itoh, H., Tomita, H., Uno Y., & Naomasa, S. (2011). Development of method for
515 nondestructive measurement of nitrate concentration in vegetable leaves by near
516 infrared spectroscopy. *IFAC Proceedings Volumes*, 44, 1773–1778.

517 Jin, X., Shi, C., Yu, C.Y., Yamada, T., & Sacks, E.J. (2017). Determination of leaf water
518 content by visible and near-infrared spectrometry and multivariate calibration in
519 *Miscanthus*. *Frontiers in Plant Science*, 8(271), 1–8.

- 520 Jones, H.G. (2004). Irrigation scheduling: advantages and pitfalls of plant-based methods.
521 *Journal of Experimental Botany*, 55, 2427–2436.
- 522 Jones, H.G. (2007). Monitoring plant and soil water status: established and novel methods
523 revisited and their relevance to studies of drought tolerance. *Journal of*
524 *Exerimental Botany*, 58, 119–130.
- 525 León, L., & Downey, G. (2006). Preliminary studies by visible and near-infrared
526 reflectance spectroscopy of juvenile and adult olive (*Olea europea* L.) leaves.
527 *Journal of the Science and Agriculture*, 86, 999–1004.
- 528 Lo Gullo, M.A., & Salleo, S. (1988). Different strategies of drought resistance in three
529 Mediterranean sclerophyllous trees growing in the same environmental
530 conditions. *New Phytologist*, 108, 267–276.
- 531 Mark, H. (2001). Data analysis: Multilinear regression and Principal Component
532 Analysis. In D.A, Burns, & E.W. Ciurczak (Eds.), *Handbook of near-infrared*
533 *analysis*, No. 8 (pp. 151–188). Florida, USA: CRC Press.
- 534 Martínez, M.L., Garrido, A., De Pedro, E.J., & Sánchez, L. (1998). Effect of sample
535 heterogeneity on NIR meat analysis: the use of the RMS statistic. *Journal of Near*
536 *Infrared Spectroscopy*, 6, 313–320.
- 537 Menesatti, P., Antonucci, F., Pallottino, F., Rocuzzo, G., Allegra, M., Stagno, F., &
538 Intrigliolo, F. (2010). Estimation of plant nutritional status by Vis–NIR
539 spectrophotometric analysis on orange leaves [*Citrus sinensis* (L) Osbeck cv
540 Tarocco]. *Biosystems Engineering*, 105, 448–454.
- 541 Mullan, D., & Pietragalla, J. (2012). Leaf relative water content. In A. Pask, J. Pietragalla,
542 D. Mullan, & M. Reynolds (Eds.), *Physiological breeding II: A field guide to*
543 *wheat phenotyping* (pp. 25-27). Mexico: CIMMYT.

544 Nevo, E., Bolshakova, M.A., Martyn, G.I., Musatenko, L.I., Sytnik, K., Pavlíček, T., &
545 Beharav, A. (2000). Drought and light anatomical adaptive leaf strategies in three
546 woody species caused by microclimatic selection at ‘Evolution Canyon’, Israel.
547 *Israel Journal of Plant Sciences*, 8, 33–46.

548 Osborne, B.G., Fearn, T., & Hindle, P. (1993). *Practical NIR spectroscopy with*
549 *applications in food and beverage analysis*. Harlow, UK: Addison-Wesley
550 Longman Ltd.

551 Pérez-Marín, D., Garrido-Varo, A., & Guerrero, J.E. (2005). Implementation of LOCAL
552 algorithm with near-infrared spectroscopy for compliance assurance in compound
553 feedingstuffs. *Applied Spectroscopy*, 59, 69–77.

554 Rallo, L., & Cuevas, J. (2017). Fructificación y producción. In D. Barranco, R.
555 Fernández-Escobar, L. Rallo (Eds.), *El cultivo del olivo* (pp. 147-189). Madrid:
556 Mundi-Prensa.

557 Rotbart, N., Schmilovitch, Z., Cohen, Y., Alchanatis, V., Erel, R., Ignat, T., Shenderay,
558 C., Dag, A., & Yermiyahu, U. (2013). Estimating olive leaf nitrogen concentration
559 using visible and near-infrared spectral reflectance. *Biosystems Engineering*, 114,
560 426–434.

561 Shenk, J.S., & Westerhaus, M.O. (1995a). *Analysis of agriculture and food products by*
562 *near infrared reflectance spectroscopy*. Silver Spring: Monograph, NIRSystems,
563 Inc.

564 Shenk, J.S., & Westerhaus, M.O. (1995b). *Routine operation, calibration, development*
565 *and network system management manual*. Silver Spring: NIRSystems, Inc.

566 Shenk, J.S., & Westerhaus, M.O. (1996). Calibration the ISI way. In A.M.C. Davies, &
567 P. Williams (Eds.), *Near infrared spectroscopy: The future waves* (pp.198-202).
568 Chichester: NIR Publications.

- 569 Shenk, J.S., Westerhaus, M.O., & Berzaghi, P. (1997). Investigation of a LOCAL
570 calibration procedure for near infrared instruments. *Journal of Near Infrared*
571 *Spectroscopy*, 5, 223–232.
- 572 Shenk, J.S., Workman, J., & Westerhaus, M. (2008). Application of NIR spectroscopy to
573 agricultural products. In D.A. Burns, & E.W. Ciurczac (Eds.), *Handbook of near*
574 *infrared analysis* (pp. 347-386). Boca Raton, FL: CRC Press, Taylor & Francis
575 Group.
- 576 Steidle-Neto, A.J., Lopes, D.C., Pinto, F.A.C., & Zolnier, S. (2017). Vis/NIR
577 spectroscopy and chemometrics for non-destructive estimation of water and
578 chlorophyll status in sunflower leaves. *Biosystems Engineering*, 155, 124–133.
- 579 Stocker, O. (1929). Das wasserdefizit von gefässpflanzen in verschiedenen klimazonen.
580 *Planta*, 7, 382–387.
- 581 Tanasijevic, L., Todorovic, M., Pereira, L.S., Pizzigalli, C., & Lionello, P. (2014).
582 Impacts of climate change on olive crop evapotranspiration and irrigation
583 requirements in the Mediterranean region. *Agricultural Water Management*, 144,
584 54–68.
- 585 Warburton, P., Brawner, J., & Meder, R. (2014). Technical Note: Handheld near infrared
586 spectroscopy for the prediction of leaf physiological status in tree seedlings.
587 *Journal of Near Infrared Spectroscopy*, 22, 433–438.
- 588 Williams, P.C. (2001). Implementation of near-infrared technology. In P.C. Williams, &
589 K.H. Norris (Eds.), *Near-infrared technology in the agricultural and food*
590 *industries* (pp. 145-169). St. Paul, MN: AACCC, Inc.
- 591 Windham, W.R., Mertens, D.R., & Barton II, F.E. (1989). Protocol for NIRS calibration:
592 sample selection and equation development and validation. In G.C. Martens, J.S.
593 Shenk, & F.E. Barton II (Eds.), *Near infrared spectroscopy (NIRS): Analysis of*

594 *Forage Quality*, No. 643 (pp. 96-103). Washington, DC: USDA-ARS, US
595 Government Printing Office.

596 Wise, B.M., Gallagher, N.B., Bro, R., Shaver, J.M., Windig, W., & Koch, R.S. (2006).
597 *PLS_ToolBox 4.0. Manual for use with MATLAB (TM)* [Computer software].
598 Wenatchee, WA: Eigenvector Research, Inc.

599 Yang, G.L., Lu, Y.L., Luo, J.Z., Wang, C.B., Meder, R., Warburton, P., & Arnold, R.J.
600 (2017). Monitoring water potential and relative water content in *Eucalyptus*
601 *camaldulensis* using Near Infrared Spectroscopy. *Journal of Tropical Forest*
602 *Science*, 29, 121–128.

603 Zhang, Q., Li., Q., & Zhang, G. (2012). Rapid determination of leaf water content using
604 VIS/NIR spectroscopy analysis with wavelength selection. *International Journal*
605 *of Spectroscopy*, 27, 93–105.

606 Zhang, Y., Luo, L., Li, J., Li, S., Qu, W., Ma, H., & Ye, X. (2017). In-situ and real-time
607 monitoring of enzymatic process of wheat gluten by miniature fiber NIR
608 spectrometer. *Food Research International*, 99, 147–154.

609

610 **Table 1 - Olive phenological stages on date analysis.**

Measurement date	Number of samples	Phenological stage	Mean temperature (°C)	Mean relative humidity (%)	Leaf RWC (%)		
					Min	Max	Mean
1. 03/16/2016	10	Bud dormancy	14.40	74.10	89.81	93.31	92.40
2. 03/30/2016	15	Flower development	16.60	61.90	89.40	93.10	92.10
3. 04/06/2016	15	Flower development	17.60	54.80	90.40	95.10	93.20
4. 04/21/2016	5	Flower development	16.30	68.60	91.50	96.20	93.50
5. 04/28/2016	15	Flower development	19.20	64.80	91.70	95.80	93.50
6. 05/04/2016	8	Flower development	20.50	41.00	86.80	93.00	90.50
7. 05/23/2016	15	Fruit set	23.00	44.40	89.80	94.80	91.30
8. 06/09/2016	16	Fruit set	29.50	42.10	85.50	89.40	91.80
9. 06/15/2016	15	Fruit set	23.30	47.80	86.90	95.60	90.70
10. 06/20/2016	15	Fruit growth	27.70	37.30	89.00	95.40	91.70
11. 06/30/2016	15	Fruit growth	28.20	50.10	86.60	95.60	92.10
12. 07/26/2016	22	End of stone hardening	32.60	31.80	83.60	90.00	87.40
13. 10/06/2016	22	Fruit ripening	24.30	52.90	77.20	88.70	84.10
14. 11/02/2017	22	Fruit ripening	18.80	67.10	84.60	92.40	89.00
15. 03/02/2017	15	Flower development	13.70	72.30	90.40	92.60	91.60
16. 03/16/2017	15	Flower development	12.70	65.60	90.90	95.50	92.40
17. 04/05/2017	10	Flower development	17.10	49.40	90.40	92.90	91.70

611

612

613

614

615 **Table 2 - MPLS regression statistics for NIR-based models for predicting RWC in**
 616 **olive leaves.**

Scatter correction	Math treatment	N	Mean	SD	SEC	r^2_c	SECV	r^2_{cv}	RPD _{cv}
SNV + DT	1,5,5,1	167	90.82	2.55	1.68	0.57	1.78	0.52	1.71
	1,10,5,1	163	90.94	2.45	1.70	0.51	1.73	0.50	1.76
	2,5,5,1	163	90.71	2.50	1.51	0.64	1.58	0.61	1.93
	2,10,5,1	164	90.84	2.45	1.63	0.56	1.68	0.53	1.82
MSC	1,5,5,1	161	90.79	2.42	1.46	0.64	1.52	0.61	2.01*
	1,10,5,1	163	90.81	2.45	1.58	0.59	1.63	0.57	1.87
	2,5,5,1	162	90.75	2.46	1.49	0.64	1.54	0.61	1.98
	2,10,5,1	166	90.85	2.54	1.82	0.49	1.86	0.47	1.64

617 * Best model for RWC prediction.

618

619 **Fig. 1 - First derivative spectra of olive leaves prior to removing the noise.**

620

621

622

623

624

625

626

627

628

629

630

631

632

633

634

635

636

637

638

639

640

641

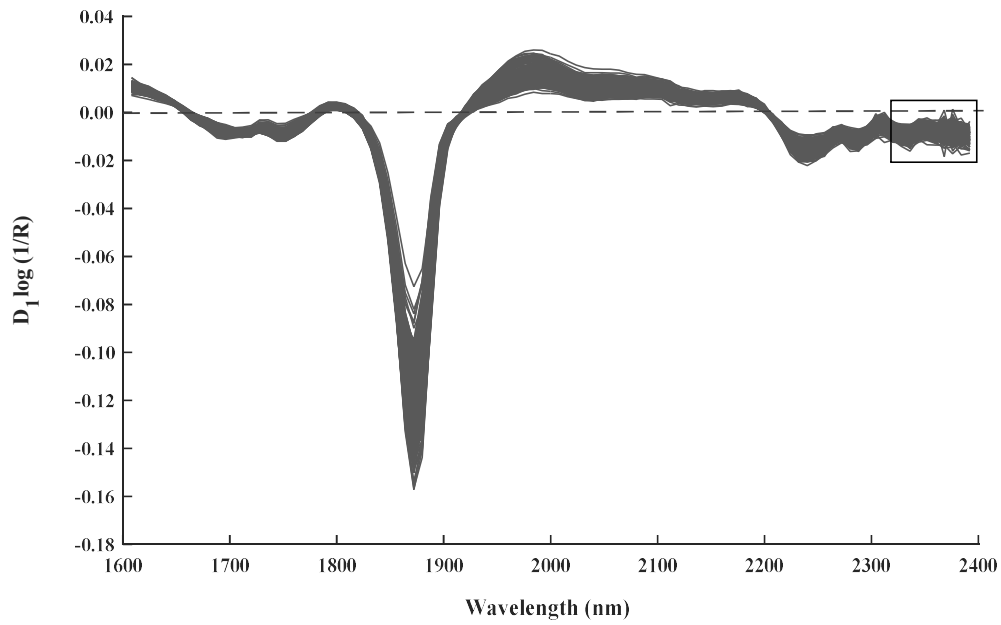
642

643

644

645

646



647 **Fig. 2 - Loadings weight (a) and score plot (b) for the second (PC2) and third (PC3)**
 648 **principal components for olive leaf spectra.**

649

650

651

652

653

654

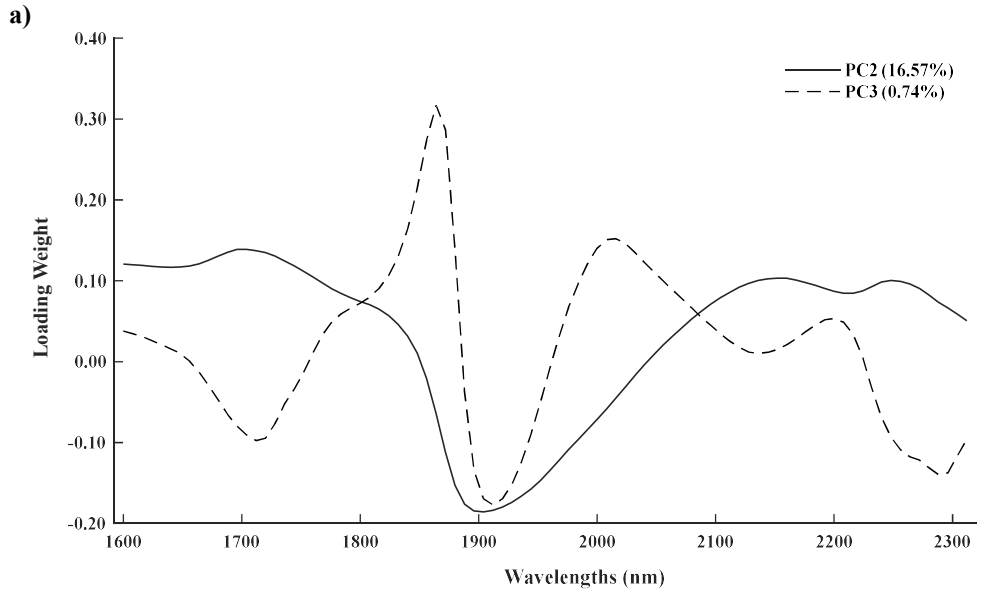
655

656

657

658

659



660

661

662

663

664

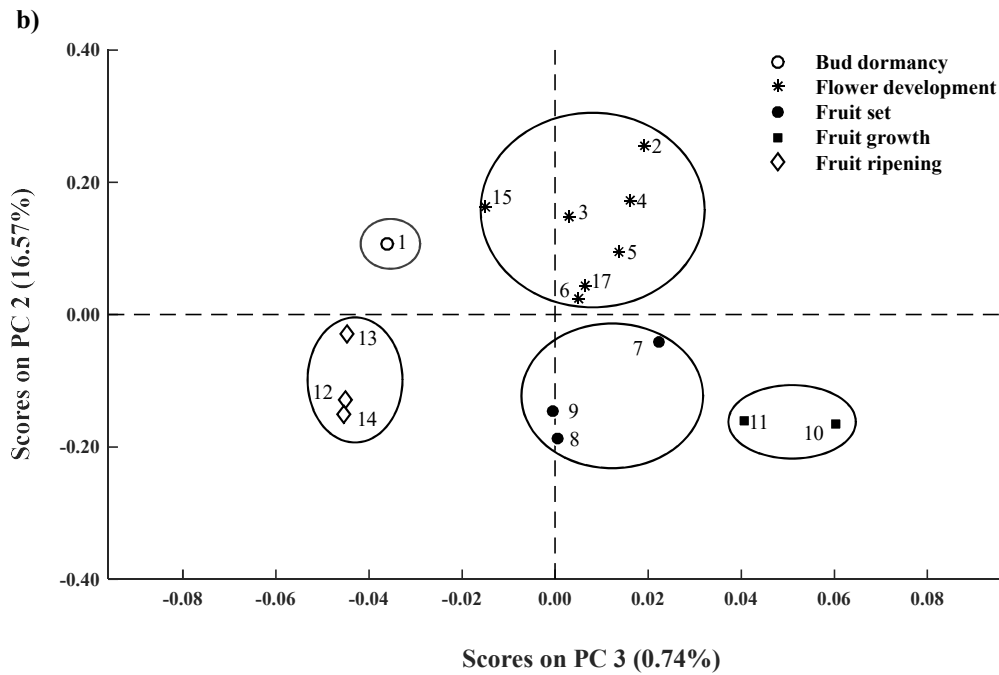
665

666

667

668

669



670

671

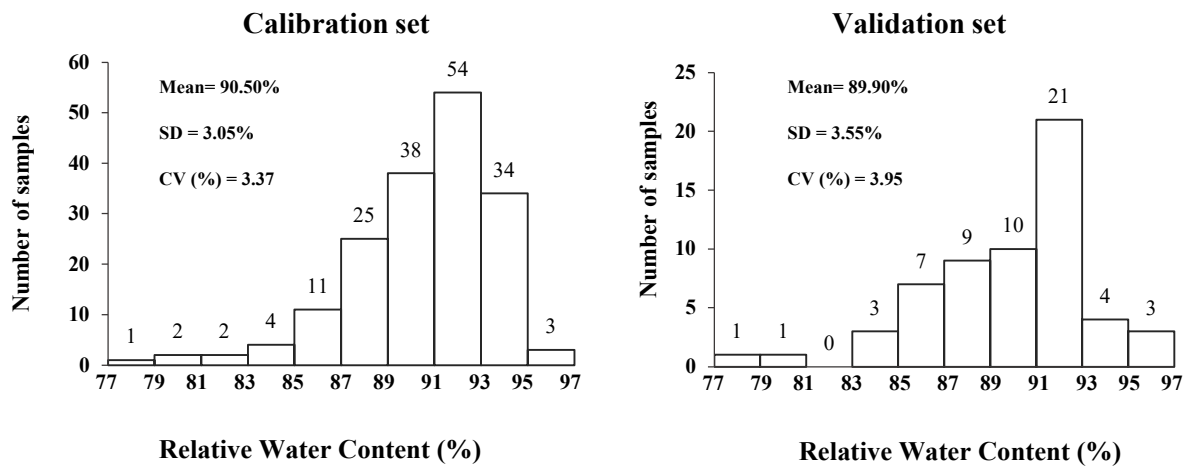
672 *More information is displayed in Table 1.

673

674

675 **Fig. 3 - Calibration and validation sets structure for the RWC.**

676



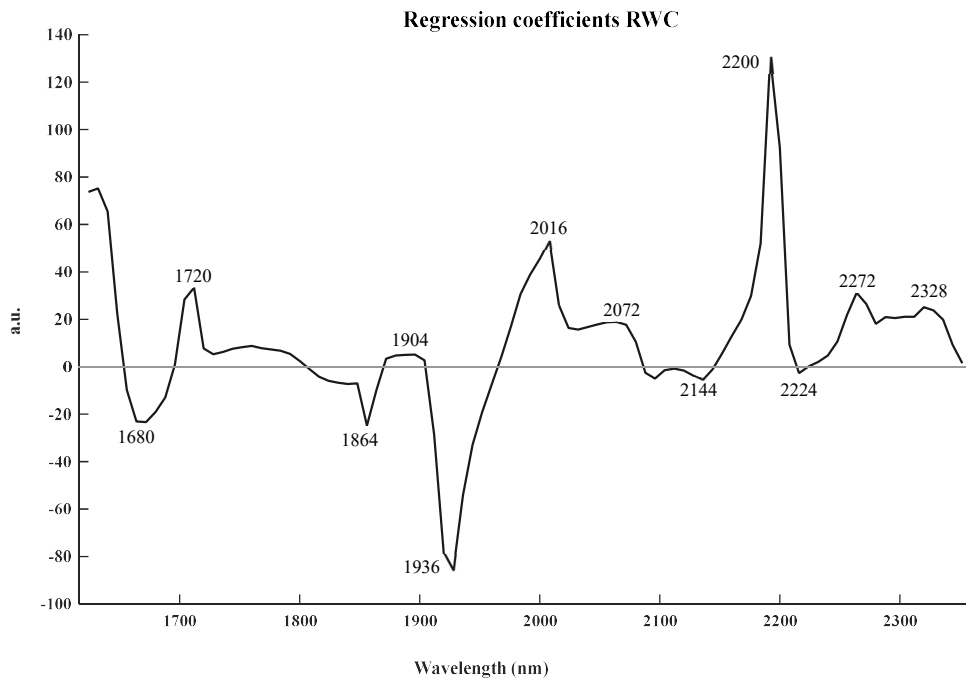
677

678

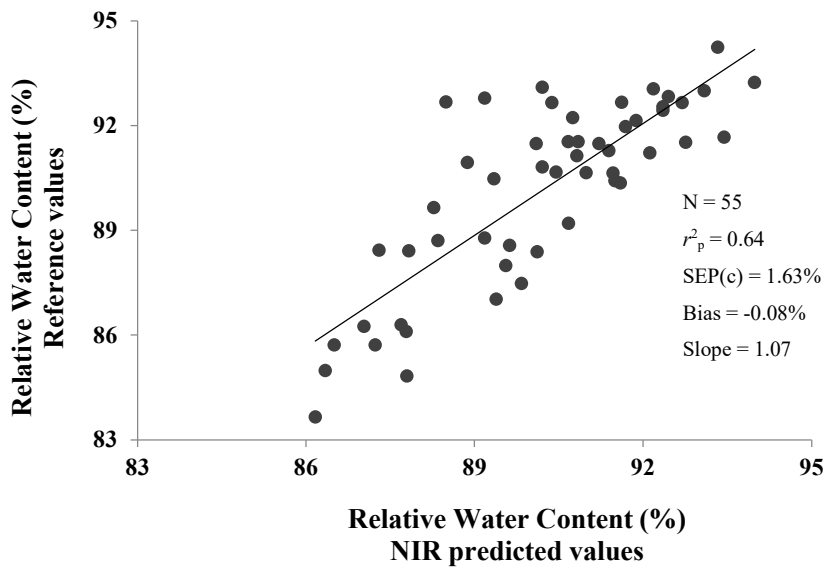
679

680 **Fig. 4 – Regression coefficients for the RWC predictive model.**

681



682 **Fig. 5 - Reference vs. NIR predicted data for the validation set.**



683